Early events induced by the toxin deoxynivalenol lead to programmed cell death in Nicotiana tabacum cells

Amine Yekkour, Daniel Tran, Delphine Arbelet-Bonnin, Joël Briand, Florence Mathieu, Ahmed Lebrihi, Rafik Errakhi, Nasserdine Sabaou, François Bouteau

Early events induced by the toxin deoxynivalenol lead to programmed cell death in *Nicotiana tabacum* cells

Amine Yekkour[a,b,c], Daniel Tran[a], Delphine Arbelet-Bonnin[a], Joël Briand[a], Florence Mathieu[d], Ahmed Lebrihi[d,e], Rafik Errakhi[e], Nasserdine Sabaou[b], François Bouteau[a,*]

[a] *Université Paris Diderot, Sorbonne Paris Cité, Institut des Energies de Demain, Paris, France*
[b] *Ecole Normale Supérieure de Kouba, Laboratoire de Biologie de Systèmes Microbiens, Alger, Algeria*
[c] *Institut National de la Recherche Agronomique d'Algérie, Centre de Recherche polyvalent Mehdi Boualem, Alger, Algeria*
[d] *Université de Toulouse, Laboratoire de Génie Chimique UMR 5503 (CNRS/INPT/UPS), ENSAT/INP de Toulouse, Castanet-Tolosan Cedex, France*
[e] *Université Moulay Ismail, Marjane 2, BP 298, Meknès, Maroc*

A B S T R A C T

Deoxynivalenol (DON) is a mycotoxin affecting animals and plants. This toxin synthesized by *Fusarium culmorum* and *Fusarium graminearum* is currently believed to play a decisive role in the fungal phytopathogenesis as a virulence factor. Using cultured cells of *Nicotiana tabacum* BY2, we showed that DON-induced programmed cell death (PCD) could require transcription and translation processes, in contrast to what was observed in animal cells. DON could induce different cross-linked pathways involving (i) reactive oxygen species (ROS) generation linked, at least partly, to a mitochondrial dysfunction and a transcriptional down-regulation of the alternative oxidase (*Aox1*) gene and (ii) regulation of ion channel activities participating in cell shrinkage, to achieve PCD.

Keywords:
Programmed cell death
Deoxynivalenol
Fusarium
Nicotiana tabacum
Ion channels

1. Introduction

Phytopathogenic *Fusarium culmorum* and *Fusarium graminearum* synthesize various mycotoxins *in planta*, including B-type sesquiterpene epoxide trichothecene, deoxynivalenol (DON). This toxin acts as a virulence factor by increasing the aggressiveness and symptoms of disease [1,2] and is also toxic to animals [3].

In animal cells, DON alters basic metabolic cell processes, including an inhibition of nucleic acid and protein synthesis by a binding to the ribosomal peptidyltransferase [3,4]. DON also induces a variety of events leading to apoptosis, such as nuclear DNA fragmentation, membrane structure and integrity disturbance, generation of reactive oxygen species (ROS) and reduction of mitochondrial transmembrane potential ($\Delta\psi_m$) [3,5,6]. Trichothecenes have effectively been shown to target mitochondria, where they can inhibit mitochondrial protein synthesis and increasing mitochondrial ROS levels [7]. In plant cells, responses to DON include alteration of cell membrane structure [8], inhibition of some enzymatic activities linked to mitochondrial functions [9], overproduction of hydrogen peroxide (H_2O_2) and PCD [10]. However, low concentrations of DON have recently been shown to inhibit the PCD induced by abiotic stress in Arabidopsis cell cultures [11]. The DON level during the infection process seems to depend on the pathogen trophic stage and participates in a sophisticated strategy to circumvent and hijack the plant's defence system [12]. Low concentrations of DON can inhibit host cell PCD during the early biotrophic phase of infection, whereas higher DON concentrations participate in the second necrotrophic phase [11–13]. Desmond et al. [10] provided evidence that DON may not only induce inhibition of protein synthesis activity. The authors demonstrated induction of a suite of defence gene transcripts and proteins in wheat seedlings. Through a priming experiment that enhanced plant defence against *F. graminearum* in wheat, DON production has also been shown to be boosted [14]. Thus, the effects of DON appear to be complex and the mechanism of toxicity remains poorly understood in plant. The intention in the present study was to further elucidate early cellular and molecular mechanisms induced in BY2 cells in response to a high level of DON and examine their

* Corresponding author at: Université Paris Diderot, Sorbonne Paris Cité, Institut des Energies de Demain, case courrier 7040 Lamarck, 75205 Paris Cedex 13, France. Tel.: +33 1 57 27 84 63.
E-mail address: francois.bouteau@univ-paris-diderot.fr (F. Bouteau).

contribution to plant cell death. We found that, in addition to ROS generation and mitochondrial dysfunction, DON-induced PCD requires regulation of ion channels participating in cell shrinkage as observed for other fungi-derived toxins such as cryptogein or oxalic acid [15,16].

2. Materials and methods

2.1. Plant cell culture conditions

Nicotiana tabacum BY2 cell suspensions were grown in Murashige and Skoog medium (MS medium) at pH 5.8 [17]. They were maintained at 22 ± 2 °C in darkness with continuous shaking at 120 rpm. Cell suspensions were sub-cultured weekly using a 1:40 dilution. All experiments were performed at 22 ± 2 °C using log-phase cells (6–7 days after sub-culture).

2.2. Cell protoplast preparation

BY2-protoplasts were isolated from suspension cultures. Two millilitre of cell suspension was used. After cell self-sedimentation (5 min), the supernatant was removed and replaced by 1 ml of fresh MS medium containing 0.02 g cellulysin, 0.01 g macerase and 0.6 M sorbitol. The digestion was carried out under shaking at 120 rpm −22 °C for 60 min. After incubation, protoplasts were collected by centrifugation at 200 rpm for 3 min and re-suspended in 1 ml of MS medium containing 0.3 M sorbitol to liberate protoplast, then centrifuged again under the same conditions. Finally, the supernatant was removed and the remaining protoplasts were re-suspended in 5 ml of fresh MS medium.

2.3. Evaluation of protoplasts volume

To determine whether DON induced a modification of protoplast volume, BY2 protoplasts exposed to DON were photographed at 15 min intervals for 3 h. The images obtained were then subjected to quantitative evaluation of the area of the protoplasts, which gave an estimation of their whole volume, on the basis of signal intensity analysis using Image J software. The area was expressed as a relative percentage (%) of the original protoplast area (at $t = 0$) in order to normalize the diversity of cell protoplast size (ranging from 20 to 100 μm).

2.4. Cell viability assay

Cell viability was assessed using the fluorescein diacetate (FDA) spectrofluorimetric method [18]. After the appropriate DON-treatment, 1 ml of cell suspension (0.05 g FW) was gently stirred with a magnetic stirrer before FDA was added at a final concentration of 12 μM. The fluorescence increase was monitored over 120 s using an F-2000 spectrofluorimeter (Hitachi, Japan). The slope obtained corresponded to the esterase activity. The results are presented as the percentage of cell death = slope of treated cells/slope of control cells × 100. Control cells were cells added with a water volume equivalent to that of the DON treatment. The time course of death for control cells was evaluated by comparing the slopes obtained with control cells at each considered time with the slope for control cells at $t = 0$. The experiment was repeated at least 3 times for each condition.

Cell and protoplast viability was also checked using the vital dyes Evans blue (EB) or neutral red (NR) after DON treatment for different time periods with or without the appropriate pharmacological effectors. Cells (50 μl) were incubated for 5 min in 1 ml phosphate buffer pH 7 supplemented with EB or NR at a final concentration of 0.005% or 0.01%, respectively. Cells that accumulated EB or did not accumulate NR were considered dead. At least 500 cells were observed and counted under a light microscope for each treatment and the experiments were repeated at least 3 times for each condition.

2.5. Measurement of reactive oxygen species production

Reactive oxygen species (ROS) release in the medium was quantified by measuring the chemiluminescence of luminol reacting with ROS [17]. Briefly, 10 ml of the *N. tabacum* BY2 cell suspension was inoculated with 50 μg ml^{-1} of DON alone or with the appropriate chemical effectors. Before measurements were made, 5 μl luminol (1.1 mM) was added to each 200 μl of cell suspension (0.05 g FW ml^{-1}). Chemiluminescence was monitored every 30 min using a FB12-Berthold luminometer (signal integrating time of 0.2 s). The measurement was repeated at least 3 times for each condition.

2.6. Aequorin luminescence measurements

Cytoplasmic Ca^{2+} variations were recorded from BY2 cell suspensions expressing the apoaequorin gene [19]. For calcium measurement, aequorin was reconstituted by an overnight incubation of the cell suspension in MS medium supplemented with 2.5 μM native coelenterazine. Cell culture aliquots (450 μl in MS; 0.05 g FW ml^{-1}) were carefully transferred to a luminometer glass tube and luminescence was recorded continuously at 0.2 s intervals using an FB12-Berthold luminometer (Berthold Technologies, Bad Wildbad, Germany). Treatments were performed by pipette injections of 50 μl containing the effectors. At the end of each experiment, residual aequorin was discharged by addition of 500 μl of a 1 M $CaCl_2$ solution dissolved in 100% methanol. The resulting luminescence was used to estimate the total amount of aequorin in each experiment. Calibration of the calcium measurement was performed using the equation: $pCa = 0.332588\,(-\log k) + 5.5593$, where k is a rate constant equal to the luminescence counts per second divided by total remaining counts. Data were expressed as μM.

2.7. Electrophysiology

Individual cells were impaled and voltage-clamped in the MS medium (main ions 28 mM NO_3^-, 16 mM K^+) using an Axoclamp 2B amplifier (Axon Instruments, Foster City, CA, USA) for discontinuous single electrode voltage clamp (dSEVC) experiments as previously described [15,20]. This allowed electrophysiological variations in living cells with their cell wall to be determined in non-stressing conditions. Voltage and current were digitized using a computer fitted with a Digidata 1320A acquisition board (Axon Instruments). The electrometer was driven by pClamp software (pCLAMP8, Axon Instruments).

2.8. Mitochondrial membrane potential measurement

The mitochondrial membrane potential was monitored using JC-1 fluorochrome [21]. Briefly, before treatment, cells were first stained with the mitochondrial membrane potential probe JC-1 by incubating 2 ml of cell suspensions (0.05 g FW ml^{-1}) for 15 min (22 °C in the dark) with 2 μg ml^{-1} JC-1 (3 μM). Treated cells were then analysed using a Hitachi F-2000 spectrofluorimeter. The excitation wavelength used was 500 nm. Fluorescence signals were collected using a band pass filter centred at 530 and 590 nm. Then, fluorescence ratios (high versus low) were evaluated. Valinomycin (a drug known to affect mitochondrial membrane potential) at 1 μM was used as a positive control.

2.9. Mitochondrial swelling assay

Mitochondria were isolated from 250 mg of BY2 cells and prepared for the assay as previously described [22]. Mitochondrial swelling was measured by the decrease in absorbance at 540 nm [23] using a 96-well plate reader (Tecan infinite^{TM} M200 spectrophotometer) with a signal integrating time of 67 s. The measurement was repeated at least 3 times for each condition.

2.10. Quantitative real-time qRT-PCR analysis of Aox1 gene expression

Seven-day-old cells were treated with DON, harvested and frozen in liquid nitrogen. Total RNA was extracted with the Trizol reagent (Invitrogen) according to the manufacturer protocol. Total RNA (2 μg) was treated with DNase I (Sigma), reverse transcribed with Revertaid Reverse Transcriptase (Fermentas) in a 25 μl reaction volume and amplified with Mastercycler ep Realplex (Eppendorf) using 5 μl of 50-fold diluted cDNA solution. Real-time PCRs were performed with the MaximaTM SYBR Green qPCR Master Mix (Fermentas) and 0.23 μM of *Aox1* primer (forw, CACCAATGATGTTGGAAACAGTG; rev, ATACCCAATTGGTGCTGGAG) [24] in a 15 μl reaction. Cycle thresholds were calculated using the Realplex 2.0 software (Eppendorf). A standard curve made with dilutions of cDNA pools was used to calculate the reaction efficiencies and the relative expression was calculated as indicated by Hellemans et al. [25] with ACT, EF1α4 and UBQ5 as reference genes [20,24]. An arbitrary value of 100 was assigned to control samples for normalization according to Pfaffl [26].

2.11. Statistics

All data were subjected to an analysis by analysis of variance (ANOVA). Mean separation was accomplished by the Newman and Keuls multiple range test and significance was evaluated at the probability level of $P \leq 0.05$.

3. Results

3.1. DON induced cell death in BY2 cell suspension

Using BY2 cell suspension as model, we found that DON was able to induce a time- and dose-dependent cell death (Fig. 1A). More than 80% of cells were dead within 8 h of treatment with DON at 10 μg ml^{-1}. When exposed to 50 or 100 μg ml^{-1} DON, this cell death level was reached after only 4 h and then levelled off to a plateau (Fig. 1A). Cell death was accompanied by a large plasma membrane retraction (Fig. 1B). Since, such cell shrinkage has been reported to be a hallmark of PCD processes [27], we analysed the shrinkage kinetic of DON-exposed protoplasts. The vital staining with NR allowed observing a fast and extensive protoplast condensation occurring before cell death (Fig. 1C). However, after 3 h of DON addition, 60% of protoplasts appeared extensively retracted (Fig. 1C and D) and dead, since NR staining disappeared (Fig. 1D). In order to confirm whether this DON-induced cell death was due to an active mechanism requiring active gene expression and cellular metabolism, BY2 cell suspensions were treated with 20 μg ml^{-1} of actinomycin D (AD) or rifampicin (Rif), inhibitors of RNA synthesis, or with 20 μg ml^{-1} of cycloheximide (Chx), gentamicin (Gen) or hygromycin-B (Hyg), inhibitors of protein synthesis, 15 min prior to DON addition. All these molecules significantly reduced the DON-induced cell death (Fig. 1E). These results suggest that this cell death could require active cell metabolism, namely gene transcription and *de novo* protein synthesis.

3.2. DON-induced cell death is dependent on delayed ion channel activations

Ion flux modulations, especially leading to cytosolic calcium variations, are among the earliest events recorded during plant–microbe interactions [28]. However, treatment of BY2 cells with DON failed to induce early cytosolic Ca^{2+} variations (Fig. 2A and B). The Ca^{2+} channel blocker, La^{3+} (50–1000 μM) also failed to reduce the DON-induced cell death (Fig. 2C), suggesting that cytosolic Ca^{2+} variations are not related to DON-induced cell death. Since we observed an important shrinkage of the DON-treated cells and protoplasts (Fig. 1B and C), we further investigated a possible regulation of anion and K^+ channels in response to DON, as these channels were already implicated in processes involving cell shrinkage during stress-induced PCD in plants [15,16,20].

The impact of the anion channel blocker 9 anthracen carboxylic acid (200 μM 9AC) or the K^+ channel blockers tetraethylamonium (10 mM $TEA^{\pm}$) and cesium (10 mM Cs^+) on the extent of the DON-induced cell death was tested. Unlike what was observed for Ca^{2+}, anion and K^+ channel blockers were able to reduce cell death (Fig. 3A) and protoplast shrinkage (Fig. 3B). This suggests that K^+ and anion channels were involved in the induced cell death. When using a discontinuous single electrode voltage clamp (dSEVC), we failed to detect significant effects of DON on ion channel activities during the first minute (data not shown). We thus examined whether the effect of the DON treatment on ion channel modulation could be delayed. For this, we impaled cells and performed dSEVC recordings at different times after DON application and compared the data recorded with those of non-treated cells (Fig. 3C). In DON-treated cells, a depolarized membrane potential (V_m) of -11.7 ± 2.5 mV ($n = 3$), compared to the control cells ($V_m = -18.6 \pm 1.6$ mV, $n = 9$), was recorded 2 h after treatment (Fig. 3D). In MS medium, the main ions are 16 mM K^+ and 28 mM NO_3^-. In these conditions, the equilibrium potential estimated for K^+, E_K is about -46 mV ($[K^+]_{out} = 16$ mM with $[K^+]_{in}$ estimated at 100 mM). The equilibrium potential estimated for NO_3^- is about -25 mV ($[NO_3^-]_{out} = 28$ mM with $[NO_3^-]_{in}$ estimated at 5 mM). As previously observed with cultured tobacco cells [15] and cultured *A. thaliana* cells [20], the occurrence of anion currents in most of the cells in their culture medium explained their mean polarization, around -20 mV, recorded in control and non-stressing conditions. However, the observed depolarization was correlated with an increase in ion current to -2.05 ± 0.2 nA (after 6 s for a pulse of -200 mV, $n = 3$), from a mean control value of -1.20 ± 0.2 nA ($n = 9$) (Fig. 3E). The DON-induced currents presented the features of slow anion channel currents [29], although some of the instantaneous current may have been ensured by fast activating anion channels as described for guard cells [30]. The DON-induced depolarization and increase in ion currents were prevented by pretreatment of the cell with the anion channel blocker 9AC (Fig. 3E), strongly reinforcing the hypothesis of an anionic nature for these currents.

Three hours after the treatment, cells were hyperpolarized by about -10 mV to -23 ± 6 mV ($n = 3$) when compared to the polarization 2 h after DON addition (Fig. 3F). The recorded currents displayed different characteristics from those recorded 2 h after DON treatment (Fig. 3G and Supplemental Fig. S1). These currents were sensitive to the K^+ channel blocker $TEA^{\pm}$ (Fig. 3G). They showed a time-dependent activation for positive voltages (Fig. 3G and Supplemental Fig. S1A) and a shift of the reversal potential in the way expected for E_K upon addition of 50 mM KCl (Supplemental Fig. S1B). These biophysical and pharmacological hallmarks are reminiscent of K^+ outward rectifying channel (KORC) characteristics reported in *Arabidopsis* cultured cells [31], although an anion component could remain in the whole current, explaining the mean polarization till far from E_K despite the activation of KORCs [32]. Thus, in response to DON, anion and K^+ channels seemed to be

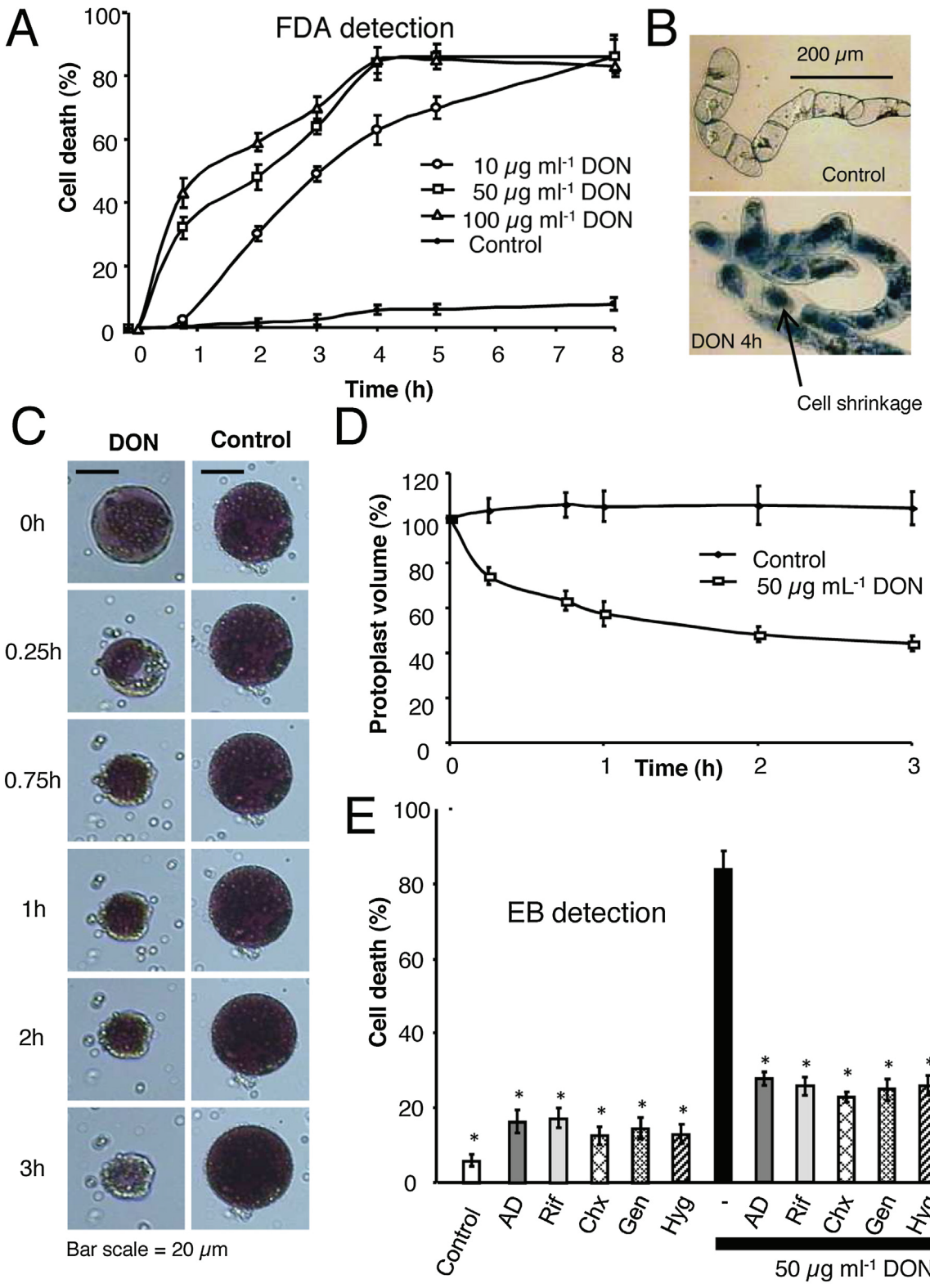

Fig. 1. DON-induced cell death in BY2 tobacco suspension culture. (A) Dose- and time- dependent development of DON-induced cell death in BY2 tobacco cells detected by the FDA technique. Cell death was induced by adding to the cells suspension 10, 50, or 100 μg ml^{-1} of DON then incubated under checking at 0, 0.75, 2, 3, 4, 5, and 8 h. (B) Light micrographs of DON-treated BY2 tobacco cells stained with Evans blue (EB). Cells were exposed to 50 μg ml^{-1} DON for 4 h. (C) Monitoring of DON (50 μg ml^{-1})-induced BY2 protoplast shrinkage. Light micrographs were taken after neutral red staining. (D) Assessment of the DON-induced decrease in protoplast volume. For volume decrease estimation (%/original volume), microscope photographs obtained in (C) were subjected to intensity analysis of area signal using Image J software. (E) Cell death extent detected by Evans blue technique after adding 50 μg ml^{-1} of DON for 4 h and effect of pretreatment with 20 μg ml^{-1} of actinomycin D (AD), rifampicin (Rif), cyclohexemide (Chx), gentamicin (Gen) and hygromycin (Hyg). For all experiments, cells treated with distilled water acted as control. The data measurements correspond to means ± SE of at least 3 independent replicates. *Significantly different from the non-pretreated cells or control ($P \leq 0.05$).

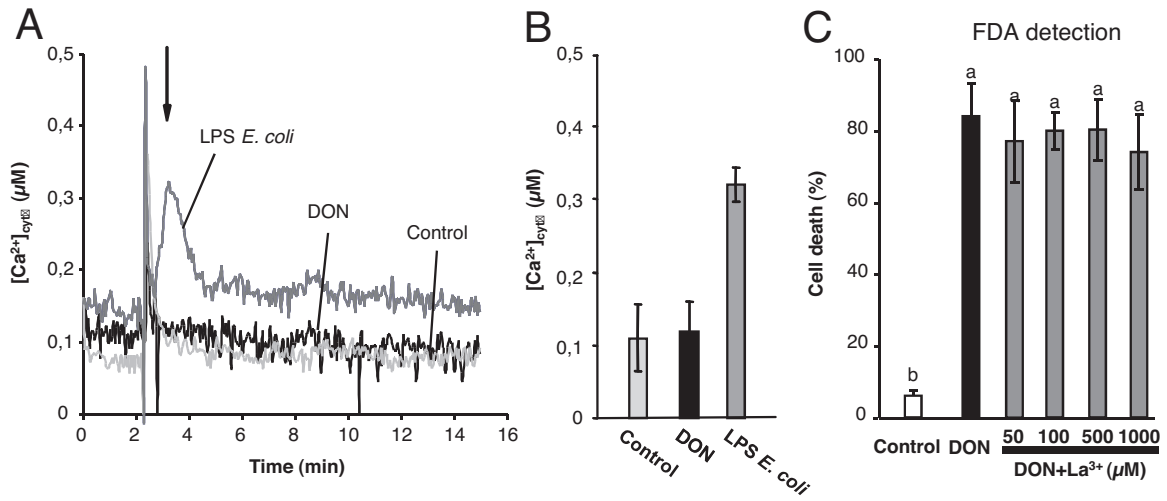

Fig. 2. Ca^{2+} is not involved in DON-induced cell death. (A) Changes in $[Ca^{2+}]_{cyto}$ were measured by using BY2 tobacco cells transformed by the apoaequorin gene treated with 50 μg ml^{-1} of DON. Treated cells with LPS *E. coli* or with distilled water were used as positive and negative control, respectively. (B) Mean values of cytosolic Ca^{2+} variation ($\Delta[Ca^{2+}]_{cyto}$) after 3 min (arrow in (A)). The data correspond to means ± SE of at least 5 independent experiments. (C) Use of La^{3+} (50–1000 μM), a plasma membrane Ca^{2+} channel inhibitor, failed to reduce DON (50 μg ml^{-1})-induced cell death after 4 h. The data reflect the means ± SE of at least 3 independent replicates. Columns with the same letters are not significantly different at $P \leq 0.05$.

successively activated in a delayed manner, leading to ion effluxes potentially involved in cell and protoplast shrinkage (Fig. 1B and C).

3.3. DON elicited a biphasic oxidative burst in BY2 cells

The generation of ROS by DON has been reported in various models [3,6,7,10]. Moreover, the most DON-productive *Fusaria* are those eliciting the greatest level of oxidative stress in ears of susceptible wheat cultivars [33]. We thus checked for the ability of DON to elicit ROS production and its impact on BY2 cell death. Addition of DON (50 μg ml^{-1}) to BY2 cells resulted in a biphasic oxidative burst (Fig. 4A). An initial increase peaked at about 1.5 h while a second peak was observed at about 3 h. Addition of 5 mM Tiron (a scavenger of O_2^-) or 10 μM diphenyleneiodonium chloride (DPI, an inhibitor of the NADPH-oxidase) significantly reduced both DON-induced ROS releases and cell death (Fig. 4B and C). This indicated that ROS, which were probably generated from O_2^- by superoxide dismutase and NADPH oxidase, play a central role in the DON-induced cell death of BY2 cells.

3.4. Mitochondrial dysfunction is involved in DON-induced cell death

Since mitochondrion is an important site for ROS production [6,34] and mitochondrial dysfunction has been reported upon DON treatment in various models [3,5,7,9], we checked the effects of DON on mitochondria and their role in DON-induced cell death. In order to discern anatomical changes, isolated mitochondria were treated with DON. DON induced a progressive decrease in absorbance at 540 nm during 2 h (Fig. 5A) reflecting the mitochondrial swelling. Since the mitochondrial swelling during the cell death processes was previously reported to be due to the formation of the mitochondrial permeability transition pore (PTP) [35], the effect of cyclosporin A (CsA), a well-known inhibitor of the PTP, was checked on the DON-induced mitochondrial swelling. This swelling seemed to be related to the formation of PTP since the addition of CsA inhibited the observed swelling. We further followed, on intact cells, the mitochondrial potential ($\Delta\psi_m$), which is known to be modified during mitochondrial swelling [35–37]. In untreated cells, the JC-1 fluorescence ratio of mitochondria displaying a high $\Delta\psi_m$ versus mitochondria presenting a low Δ_m was largely >1 (Fig. 5B). This ratio decreased in a time-dependent manner upon addition of 50 μg ml^{-1} DON indicating that DON induced a significant decrease of $\Delta\psi_m$ in most mitochondria (Fig. 5B). As observed for mitochondrial swelling (Fig. 5A), pretreatment with CsA reduced the DON-induced mitochondrial depolarization and was able to maintain $\Delta\psi_m > 1$ throughout all the experiment time courses (Fig. 5B). Such pretreatment also reduced the induced cell death by more than 50% (Fig. 5C). This indicates that the PTP opening is involved in the DON-induced mitochondrial dysfunction, and is a component of a pathway leading to DON-induced cell death.

3.5. DON reduced Aox1 gene expression

Alternative oxidase (AOX) is an enzyme involved in the antioxidant regulatory mechanism (alternative respiration pathway) of the mitochondrion by transferring electrons directly from the reduced forms of ubiquinone to O_2 [38]. AOX is known to help maintain the electron flux and to reduce ROS levels when electron transport, in the cytochrome c pathway, is blocked by stress conditions [39]. The overexpression of *Aox1*, a nuclear gene encoding AOX, has already been proved to lead to a large increase in AOX protein and alternative pathway capacity, and also to alleviate mitochondria-dependent programmed cell death [40–42]. In view of the ROS generation and mitochondrial dysfunction observed in response to DON, we checked for the relative *Aox1* transcript level in response to this toxin. The DON (50 μg ml^{-1}) significantly reduced *Aox1* transcript level within 30 min (Fig. 6). Subsequently, the mRNA level of *Aox1* increased for up to 2 h after DON addition, then reached a level representing approximately 50% of the control *Aox1* transcript expression level (Fig. 6).

4. Discussion

Using BY2 cells we showed that DON induced drastic cell death, which could also be observed on tobacco leaves (Supplemental Fig. S2). This death was preceded by a large protoplast shrinkage considered by some authors as a hallmark of PCD processes in both plant and animal cells [27,43–45]. The delineation between the different PCD types sometimes remains difficult [46]. However, upon

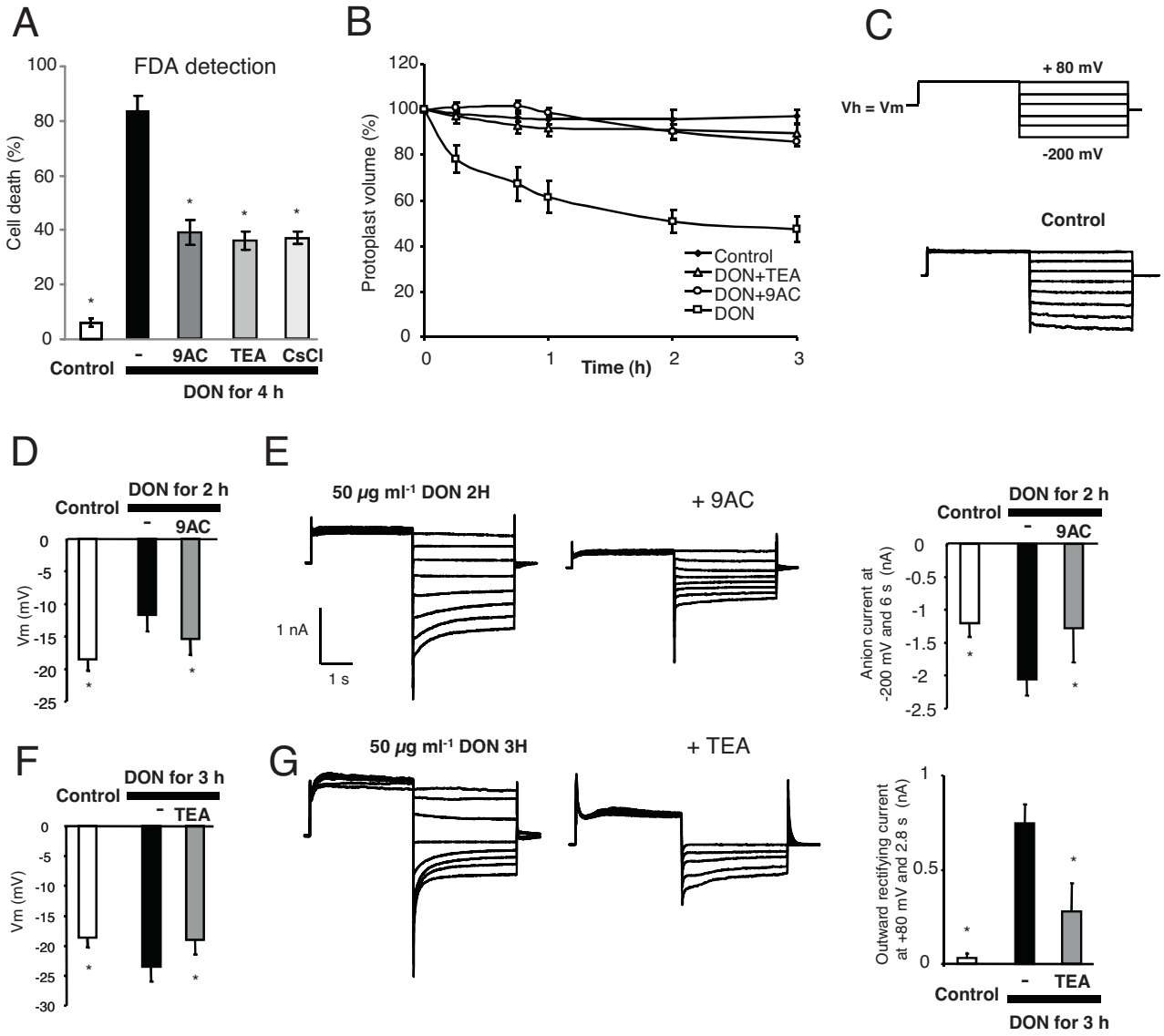

Fig. 3. DON-induced changes in plasma membrane potential and ion currents in BY2 tobacco cells. (A) Effects of anion channel inhibitor 9AC (200 μM) and K^+ channel inhibitors $TEA^{\pm}$ (10 mM) and Cs^+ (10 mM) on the induced cell death after 4 h of DON (50 μg ml^{-1}) addition. (B) Decrease in DON-induced protoplast shrinkage after addition of anion channel inhibitor 9AC (200 μM) and K^+ channel inhibitor $TEA^{\pm}$ (10 mM). (C) Ion currents measured under control conditions without DON. The protocol was as illustrated, holding potential (V_h) was V_m. (D) Mean values for PM potentials 2 h after addition of DON (50 μg ml^{-1}) with or without 9AC (200 μM). (E) Anion current recorded 2 h after addition of DON (50 μg ml^{-1}) with or without 9AC. Mean values 2 h after addition of DON (50 μg ml^{-1}) for anion currents (at 6 s for the voltage pulse of −200 mV). (F) Mean values for PM potentials 3 h after addition of DON (50 μg ml^{-1}) with or without $TEA^{\pm}$ (10 mM). (G) Time-dependent outward currents measured 3 h after addition of DON (50 μg ml^{-1}) with or without $TEA^{\pm}$ (10 mM). Mean values 3 h after addition of DON (50 μg ml^{-1}) for outward rectifying K^+ currents (at 2.8 s for the voltage pulse of +80 mV) with or without $TEA^{\pm}$. For all experiments, cells treated with distilled water acted as control. The data measurements correspond to means ± SE of at least 3 independent replicates. *Significantly different from the non-pretreated cells or control ($P \leq 0.05$).

DON treatment, we observed the transcription of HSR203J (Supplemental Fig. S3), a possible indicator of HR response [47], which is a form of PCD. We further observed a decrease in DON-induced cell death upon pretreatement with inhibitors of transcription (AD and Rif) or translation (Chx, Gen and Hyg), suggesting that DON could require active gene expression and *de novo* protein synthesis to induce cell death. The DON-induced PCD observed in BY2 cells is in agreement with results previously described for wheat [10] and animal cells [6,48,49]. However, in some animal cells, the DON toxicity seems to be dependent on an inhibition of nucleic acid and protein synthesis via the binding of DON to the ribosomal peptidyltransferase [3,4]. These data suggest that in plants, DON induces an active cell death which could proceed through other mechanisms than deregulation of transcription or translation.

Among events related to DON effects, ROS generation has been evidenced in plant [10] and animal cells [6]. Reactive oxygen species have been proposed as key inducers of different types of developmental and environmental PCD [50,51]. With BY2 cells we recorded biphasic ROS generation, as often observed in plant–pathogen interactions, where the second high intensity phase corresponds to host recognition and HR response [52,53]. The impact of the NADPH-oxidase inhibitor DPI suggested that at least some of the ROS were produced by NADPH-oxidase in response to DON. Plasma membrane NADPH oxidase, generating O_2^- in the apoplast, has been characterized in several plant species as an essential ROS-producing enzyme activated during the early stages of plant–pathogen interactions [52,54]. As expected from these data, a significant inhibition of the DON-induced cell death was found after the addition of DPI. However, since the O_2^- scavenger tiron was

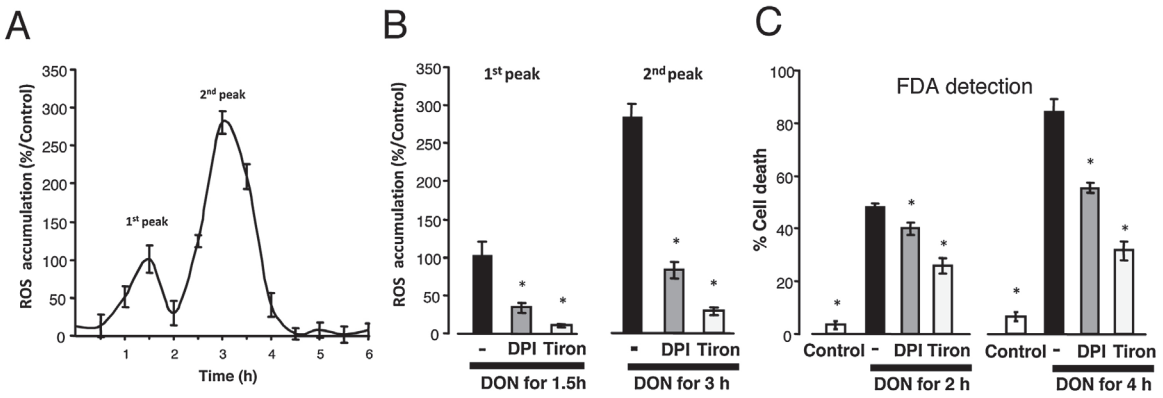

Fig. 4. DON-induced ROS production in BY2 tobacco cells. (A) H_2O_2 accumulation (%/control) in the medium of cells treated with DON (50 μg ml^{-1}). Measures were taken each 30 min for up to 6 h. (B) Percentage of variation of H_2O_2 accumulation (%/control) at 1.5 and 3 h, in the medium of cells treated with DON (50 μg ml^{-1}) and effect of pretreatment with NADPH-oxidase inhibitors DPI (10 μM) or O_2^- scavenger Tiron (5 mM) on H_2O_2 production. (C) Cell death extent detected by FDA technique after adding 50 μg ml^{-1} DON for 2 or 4 h and effect of pretreatment with DPI (10 μM) or Tiron (5 mM) on cell death. The control corresponds to cells treated with distilled water. The data correspond to means ± SE of at least 3 independent replicates. *Significantly different from the non-pretreated cells or control ($P \leq 0.05$).

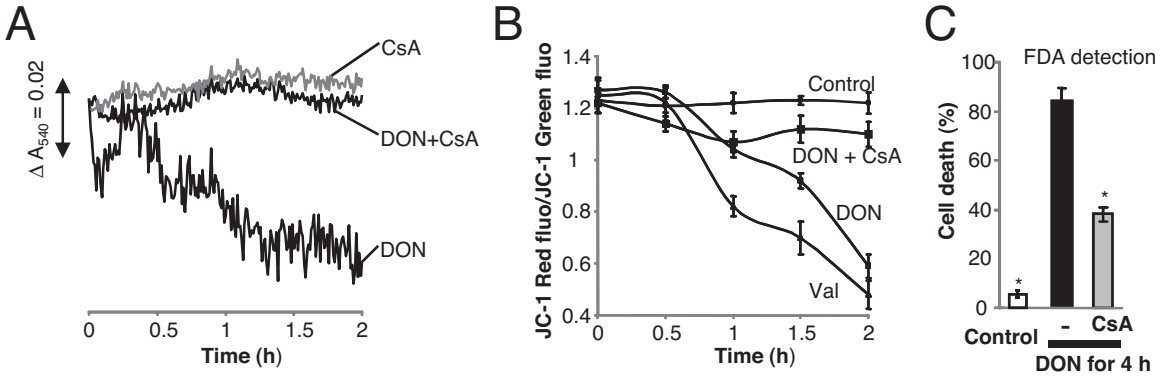

Fig. 5. DON induced mitochondrial dysfunctions in BY2 tobacco cells. (A) DON induced swelling in isolated BY2 mitochondrial. Data express relative variation in absorbance (/control) recorded at 540 nm (ΔA_{540}). The decrease in relative absorbance reflects the mitochondrial swelling. The control corresponds to mitochondria treated with distilled water. Fifty micro molar of cyclosporine A (CsA) was used to check PTP sensitiveness. The data are representative of 3 independent experiments. (B) DON induced mitochondrial membrane potential ($\Delta\psi_m$) dysfunction. The JC-1 fluorescence ratio (high ψ_m versus low ψ_m) was measured each 30 min for up to 2 h after DON (50 μg ml^{-1}) treatment. Effect of 50 μM cyclosporine A (CsA) on DON-induced decrease of JC-1 fluorescence ratio. The K^+ ionophore valinomycin (Val, 1 μM) and distilled water were used as positive and negative control, respectively. The data reflect the means ± SE of at least 4 independent experiments. (C) Effect of 50 μM CsA on cell death induced by 50 μg ml^{-1} DON estimated with FDA technique. The data reflect the means ± SE of at least 3 independent replicates. *Significantly different from the non-pretreated cells or control ($P \leq 0.05$).

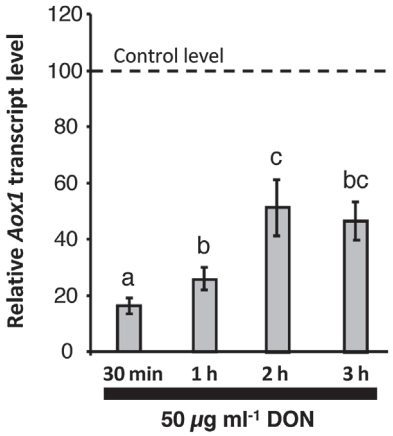

Fig. 6. Effect of DON on alternative oxidase (*Aox1*) gene expression in BY2 tobacco cells. Quantitative reverse transcriptase polymerase chain reaction (qRT-PCR) was performed with RNA extracted 30 min, 1, 2, or 3 h after addition of DON (50 μg ml^{-1}). Columns with the same letters are not significantly different at $P \leq 0.05$.The relative expression was calculated with reference to ACT, EF1α4 and UBQ5 genes. An arbitrary value of 100 was assigned to control samples (cells treated with distilled water) for normalization. The data reflect the means ± SE of at least 3 independent replicates.

more potent than DPI to decrease the DON-induced ROS levels and cell death, the presence of other source(s) of ROS can be suspected. Among various sources, dysfunction of mitochondria in plants, as in animals, could induce large amounts of ROS [6,34]. Dysfunction of mitochondria through PTP opening is also considered as a major determinant in the cellular commitment to death [36,55,56]. In response to DON we recorded a time-dependent swelling and depolarization of the mitochondrion clearly indicating mitochondrial dysfunction. This mitochondrial swelling, decrease in $\Delta\psi_m$, and the cell death were largely attenuated in the presence of CsA, a blocker of PTP [36,37,57] as already observed in different environmentally and developmentally regulated cell death [5,17]. It is noteworthy that CsA was also efficient in decreasing DON-induced ROS generation (Supplemental Fig. S4), suggesting that ROS generation effectively accompanied mitochondrial dysfunction.

An early down regulation of *Aox1* transcription was also suspected. This DON-induced decrease in *Aox1* transcripts could occur through mitochondria-to-nucleus signalling referred to as retrograde communication [58,59] and could induce an increase in mitochondrial ROS. It is assumed that plants can induce mitochondrial AOX activity to prevent ROS overgeneration by lowering the ubiquinone reduction level [60,61], thus reducing redox stress and ROS accumulation [62]. An early superoxide burst in the

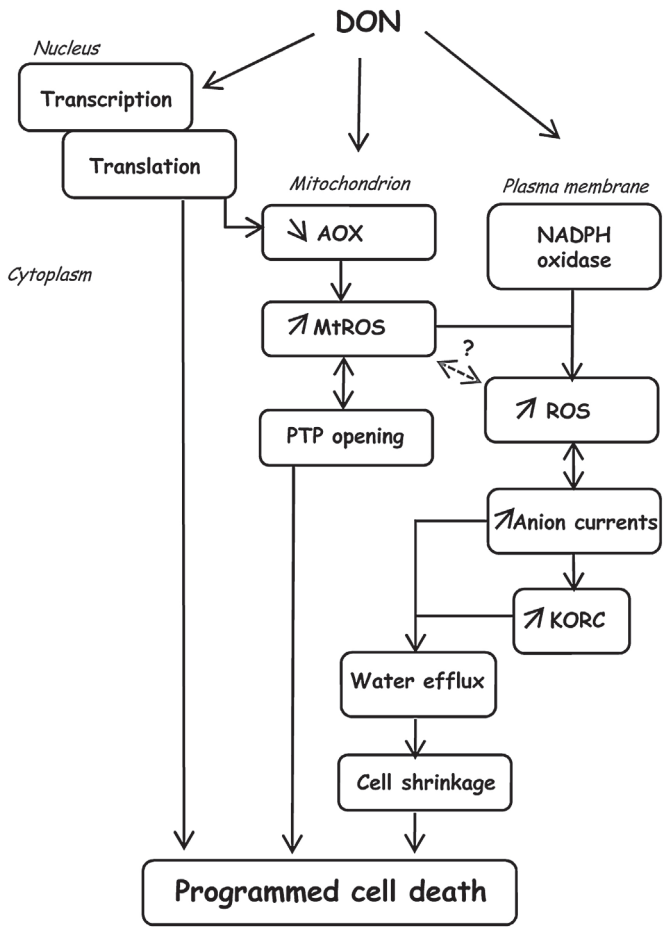

Fig. 7. Possible pathways induced by DON and leading to cell death of BY2 cells.

mitochondrial matrix preceding the HR has been reported to be due to a coordinated response of AOX [63,64]. Consistently, down-regulation of AOX level, either via inhibitors or via transgenic approaches, has been reported to cause an increase in ROS production [65] and stimulate PCD [66], while overexpression of *Aox1* has been shown to decrease PCD [42]. The partial recovery *Aox1* transcripts observed 2 h after DON treatment could be related to the 20% of surviving cells. Several studies show that AOX is involved subsequently to mitochondrial electron-transport chain dysfunction, and cells that are incapable of inducing AOX initiate a cell death response [64,67,68]. Accordingly, pretreatment of BY2 cells with pharmacological inhibitors found to affect ROS generation, ion channel activations, or mitochondrial dysfunction, induced a recovery of *Aox1* transcripts (Supplemental Fig. S5).

The DON-induced PCD was also preceded by cell shrinkage correlated to the delayed activation of anion and outward rectifying K^+ channels (KORC) by DON. The activation of anion channels appears important since the anion channel blockers 9AC decreased the DON-induced PM depolarization, anion channel increase, cell shrinkage and death. Pretreatment of cells with 9AC also reduced the DON-induced O_2^- production (Supplemental Fig. S6). The anion channel activation could amplify the DON signal by activating a NADPH-oxidase and participate in the 2nd phase of ROS generation, as already described in plant [69] and animal cells [70]. Although a little delayed, the activation of KORC also seemed important since the channel blockers $TEA^{\pm}$ and CsCl also reduced the DON-induced KORC, cell shrinkage and death. It is noteworthy that anion currents as well as KORC could be activated in response to ROS [20]. This delayed increase in KORC could also be evoked to counterbalance the depolarization of PM mediated by DON-induced anion current, allowing a partial repolarization of cells by tending to clamp V_m at E_K [71]. However, a combined efflux of anions and K^+ would drive water efflux, leading to cell shrinkage. In various mammalian cell types, apoptosis volume decrease (AVD), which is mediated by water loss caused by activation of anion channels and KORCs, is an early prerequisite for apoptotic events including cell shrinkage, ultimately leading to PCD [43]. More surprisingly, the lack of intracellular Ca^{2+} variations and the failure of La^{+3} to reduce death suggest that DON-induced death of BY2 cells is not calcium-mediated. Although Ca^{2+} influx is frequently associated with plant response and cell death [72], calcium-independent pathways have already been reported in biotic- and abiotic-stress-induced BY2 cell death [17,73].

When considering the kinetics of the events recorded in the present work, mitochondrial dysfunction, possibly through ROS generation due to decrease in AOX activity, seems to be one of the earliest major factors leading to DON-induced PCD (Fig. 7). Mitochondrial dysfunction in plants can both be caused by ROS production and result in ROS production [58]. From our data, it is difficult to know if ROS generation through NADPH-oxidase participates in mitochondrial dysfunction or constitutes a parallel ROS generation pathway. It is noteworthy that the presence of different kinds of ROS and different sites of ROS production makes understanding the ROS signalling network very difficult, notably during PCD [50]. Further studies are needed to unravel this question. However, as in animals, PTP opening in plants is proposed to allow releasing factors that trigger PCD [37] and it seems that the ROS generation could induce a second pathway involving ion channel activations leading to cell shrinkage and finally death (Fig. 7).

Acknowledgements

The authors acknowledge financial support for this work from the Agence Universitaire de la Francophonie to AY. We also thank Dr. Backer S. for help in English language editing.

References

[1] H. Hestbjerg, G. Felding, S. Elmholt, Fusarium culmorum infection of barley seelings: correlation between aggressiveness and deoxynivalenol content, J. Phytopathol. 150 (2002) 308–316.
[2] C. Jansen, D. von Wettstein, W. Schäfer, K.H. Kogel, A. Felk, F.J. Maier, Infection patterns in barley and wheat spikes inoculated with wild-type and trichodiene synthase gene disrupted *Fusarium graminearum*, PNAS 102 (2005) 16892–16897.
[3] O. Rocha, K. Ansari, F.M. Doohan, Effects of trichothecene mycotoxins on eukaryotic cells: a review, Food Addit. Contam. 22 (2005) 5369–5378.
[4] J.J. Pestka, H.R. Zhou, Y. Moon, Y.J. Chung, Cellular and molecular mechanisms for immune modulation by deoxynivalenol and other trichothecenes: unravelling a paradox, Toxicol. Lett. 153 (2004) 61–73.
[5] F. Bensassi, C. Gallerne, O. Sharaf El Dein, C. Lemaire, M. Rabeh Hajlaoui, H. Bacha, Involvement of mitochondria-mediated apoptosis in deoxynivalenol cytotoxicity, Food Chem. Toxicol. 50 (2012) 1680–1689.
[6] X. Zhang, L. Jiang, C. Geng, J. Cao, L. Zhong, The role of oxidative stress in deoxynivalenol-induced DNA damage in HepG2 cells, Toxicon 54 (2009) 513–518.
[7] M.A. Bin-Umer, J.E. McLaughlin, M.S. Butterly, S. McCormick, N.E. Tumer, Elimination of damaged mitochondria through mitophagy reduces mitochondrial oxidative stress and increases tolerance to trichothecenes, PNAS 111 (2014) 11798–11803.
[8] Z. Kang, H. Buchenauer, Immunocytochemical localization of *Fusarium* toxins in infected wheat spikes by *Fusarium culmorum*, Physiol. Mol. Plant Pathol. 55 (1999) 275–288.
[9] F. Cossette, J.D. Miller, Phytotoxic effect of deoxynivalenol and gibberella ear rot resistance of corn, Nat. Toxins 3 (1995) 383–388.

[10] O.J. Desmond, J.M. Manners, The *Fusarium* mycotoxin deoxynivalenol elicits hydrogen peroxide production, programmed cell death and defence responses in wheat, Mol. Plant 9 (2008) 435–445.
[11] M. Diamond, T.J. Reape, O. Rocha, S.M. Doyle, J. Kacprzyk, F.M. Doohan, P.F. McCabe, The fusarium mycotoxin deoxynivalenol can inhibit plant apoptosis-like programmed cell death, PloS One 8 (2013) e69542.
[12] K. Audenaert, A. Vanheule, M. Höfte, G. Haesaert, Deoxynivalenol: a major player in the multifaceted response of Fusarium to its environment, Toxins 6 (2014) 1–19.
[13] K. Kazan, D.M. Gardiner, J.M. Manners, On the trail of a cereal killer: recent advances in *Fusarium graminearum* pathogenomics and host resistance, Mol. Plant Pathol. 13 (2012) 399–413.
[14] M. Ameye, K. Audenaert, N. De Zutter, K. Steppe, L. Van Meulebroek, L. Vanhaecke, D. De Vleesschauwer, G. Haesaert, G. Smagghe, Priming of wheat with the green leaf volatile z-3-hexenyl acetate enhances defense against *Fusarium graminearum* but boosts deoxynivalenol production, Plant Physiol. 167 (2015) 1671–1684.
[15] A. Gauthier, O. Lamotte, D. Reboutier, F. Bouteau, A. Pugin, D. Wendehenne, Cryptogein-induced anion effluxes: electrophysiological properties and analysis of the mechanisms through which they contribute to the elicitor-triggered cell death, Plant Signal. Beh. 2 (2007) 89–98.
[16] R. Errakhi, P. Meimoun, A. Lehner, G. Vidal, J. Briand, F. Corbineau, J.P. Rona, F. Bouteau, Anion channel activity is necessary to induce ethylene synthesis and programmed cell death in response to oxalic acid, J. Exp. Bot. 59 (2008) 3121–3129.
[17] E. Monetti, T. Kadono, D. Tran, E. Azzarello, D. Arbelet-Bonnin, B. Biligui, J. Briand, T. Kawano, S. Mancuso, F. Bouteau, Deciphering early events involved in hyperosmotic stress-induced programmed cell death in tobacco BY-2 cells, J. Exp. Bot. 65 (2014) 1361–1375.
[18] D. Reboutier, C. Frankart, J. Briand, B. Biligui, J.P. Rona, M. Haapalainen, M.A. Barny, F. Bouteau, Antagonistic Action of Harpin Proteins: HrpWea from *Erwinia Amylovora* Suppresses HrpNea-induced Cell Death in *Arabidopsis thaliana*, J. Cell Sci. 120 (2007) 3271–3278.
[19] N. Pauly, M.R. Knight, P. Thuleau, A. Graziana, S. Muto, R. Ranjeva, C. Mazarsa, The nucleus together with the cytosol generates patterns of specific cellular calcium signatures in tobacco suspension culture cells, Cell Calcium 30 (2001) 413–421.
[20] D. Tran, H. El-Maarouf-Bouteau, M. Rossi, B. Biligui, J. Briand, T. Kawano, S. Mancuso, F. Bouteau, Post-transcriptional regulation of GORK channels by superoxide anion contributes to increases in outward-rectifying K^+ currents, New Phytologist 198 (2013) 1039–1048.
[21] R. Errakhi, A. Dauphin, P. Meimoun, A. Lehner, D. Reboutier, P. Vatsa, J. Briand, K. Madiona, J.P. Rona1, M. Barakate, D. Wendehenne, C. Beaulieu, F. Bouteau, An early Ca^{2+} influx is a prerequisite to thaxtomin a-induced cell death in *Arabidopsis thaliana* cells, J. Exp. Bot. 59 (2008) 4259–4270.
[22] D. Trono, M. Soccio, M.N. Laus, D. Pastore, The existence of phospholipase A2 activity in plant mitochondria and its activation by hyperosmotic stress in durum wheat (*Triticum durum* Desf.), Plant Sci. 199 (2013) 91–102.
[23] K. Zhao, G.M. Zhao, D. Wu, D.Y. Soong, A.V. Birk, P.W. Schiller, H.H. Szeto, Cell permeable peptide antioxidants targeted to inner mitochondrial membrane inhibit mitochondrial swelling, oxidative cell death, and reperfusion injury, J. Biol. Chem. 279 (2004) 34682–34690.
[24] T. Koshiba, M. Kobayashi, A. Ishihara, T. Matoh, Boron nutrition of cultured tobacco BY-2 cells. VI. Calcium is involved in early responses to boron deprivation, Plant Cell Physiol. 51 (2010) 323–327.
[25] J. Hellemans, G. Mortier, A. De Paepe, F. Speleman, J. Vandesompele, qBase relative quantification framework and software for management and automated analysis of real-time quantitative PCR data, Genome Biol. 8 (2007) R19.
[26] M.W. Pfaffl, A new mathematical model for relative quantification in realtime RT-PCR, Nucleic Acids Res. 29 (2001) e45.
[27] T.J. Reape, P.F. McCabe, Commentary: the cellular condensation of dying plant cells: programmed retraction or necrotic collapse? Plant Sci. 207 (2013) 135–139.
[28] W. Ma, Roles of Ca^{2+} and cyclic nucleotide gated channel in plant innate immunity, Plant Sci. 181 (2011) 342–346.
[29] J.I. Schroeder, B.U. Keller, Two types of anion channel currents in guard cells with distinct voltage regulation, PNAS 89 (1992) 5025–5029.
[30] R. Hedrich, H. Busch, K. Raschke, Ca^{2+} and nucleotide dependent regulation of voltage dependent anion channels in the plasma membrane of guard cells, EMBO J. 9 (1990) 3889–3892.
[31] E. Jeannette, J.P. Rona, F. Bardat, D. Cornel, B. Sott, E. Miginiac, Induction of RAB18 gene expression and activation of KC outward rectifying channels depend on extracellular perception of ABA in *Arabidopsis thaliana* suspension cells, Plant J. 18 (1999) 13–22.
[32] D. Reboutier, M. Bianchi, M. Brault, C. Roux, A. Dauphin, J.P. Rona, V. Legue, F. Lapeyrie, F. Bouteau, The indolic compound hypaphorine produced by ectomycorrhizal fungus interferes with auxin action and evokes early responses in nonhost *Arabidopsis thaliana*, Mol. Plant Microbe Interact. 15 (2002) 932–938.
[33] A. Waśkiewicz, I. Morkunas, W. Bednarski, V.C. Mai, M. Formela, M. Beszterda, H. Wiśniewska, P. Goliński, Deoxynivalenol and oxidative stress indicators in winter wheat inoculated with *Fusarium graminearum*, Toxins 6 (2014) 575–591.
[34] C. Gao, D. Xing, L. Li, L. Zhang, Implication of reactive oxygen species and mitochondrial dysfunction in the early stages of plant programmed cell death induced by ultraviolet-C overexposure, Planta 227 (2008) 755–767.
[35] A. Vianello, M. Zancani, C. Peresson, E. Petrussa, V. Casolo, J. Krajnakova, S. Patui, E. Braidot, F. Macri, Plant mitochondrial pathway leading to programmed cell death, Physiol. Plantarum 129 (2007) 242–252.
[36] D.C. Scott, Logan, Mitochondrial morphology transition is an early indicator of subsequent cell death in Arabidopsis, New Phytol. 177 (2008) 90–101.
[37] A. Vianello, V. Casolo, E. Petrussa, C. Peresson, S. Patui, A. Bertolini, S. Passamonti, E. Braidot, M. Zancani, The mitochondrial permeability transition pore (PTP)—an example of multiple molecular exaptation, Biochim. Biophys. Acta 1817 (2012) 2072–2086.
[38] G. Noctor, R.D. Paepe, C.H. Foyer, Mitochondrial redox biology and homeostasis in plants, Trends Plant Sci. 12 (2006) 125–134.
[39] W.C. Plaxton, F.E. Podesta, The functional organization and control of plant respiration, Crit. Rev. Plant Sci. 25 (2006) 159–198.
[40] D.P. Maxwell, Y. Wang, L. McIntosh, The alternative oxidase lowers mitochondrial reactive oxygen production in plant cells, PNAS-Biol. 96 (1999) 8271–8276.
[41] G.C. Vanlerberghe, Alternative oxidase: a mitochondrial respiratory pathway to maintain metabolic and signaling homeostasis during abiotic and biotic stress in plants, Int. J. Mol. Sci. 14 (2013) 6805–6847.
[42] J. Liu, Z. Li, Y. Wang, D. Xing, Overexpression of alternative oxidase 1a alleviates mitochondria-dependent programmed cell death induced by aluminium phytotoxicity in Arabidopsis, J. Exp. Bot. 65 (2014) 4465–4478.
[43] Y. Okada, T. Shimizu, E. Maeno, S. Tanabe, X. Wang, N. Takahashi, Volume- sensitive chloride channels involved in apoptotic volume decrease and cell death, J. Membr. Biol. 209 (2006) 21–29.
[44] E. Burbridge, M. Diamond, P.J. Dix, P.F. McCabe, Use of cell morphology to evaluate the effect of a peroxidase gene on the cell death induction thresholds in tobacco, Plant Sci. 172 (2007) 853–860.
[45] T.J. Reape, P.F. McCabe, Apoptotic-like programmed cell death in plants, New Phytol. 180 (2008) 13–26.
[46] W.G. van Doorn, E.P. Beers, J.L. Dangl, V.E. Franklin-Tong, P. Gallois, I. Hara-Nishimura, A.M. Jones, M. Kawai-Yamada, E. Lam, J. Mundy, L.A.J. Mur, M. Petersen, A. Smertenko, M. Taliansky, F. Van Breusegem, T. Wolpert, E. Woltering, B. Zhivotovsky, P.V. Bozhkov, Morphological classification of plant cell deaths, Cell Death Differ. 18 (2011) 1241–1246.
[47] D. Pontier, C. Balague, I.B. Marion, M. Tronchet, L. Deslandes, D. Roby, Identification of a novel pathogen-responsive element in the promoter of the tobacco gene HSR203 J, a molecular marker of the hypersensitive response, Plant J. 26 (2001) 495–507.
[48] R.H. Du, J.T. Cui, T. Wang, A.H. Zhang, R.X. Tan, Trichothecin induces apoptosis of HepG2 cells via caspase-9 mediated activation of the mitochondrial death pathway, Toxicon 59 (2012) 143–150.
[49] F. Bensassi, E. El Golli-Bennour, S. Abid-Essefi, C. Bouaziz, M. Rabeh Hajlaoui, H. Bacha, Pathway of deoxynivalenol-induced apoptosis in human colon carcinoma cells, Toxicology 264 (2009) 104–109.
[50] M.C. De Pinto, V. Locato, L. De Gara, Redox regulation in plant programmed cell death, Plant Cell Environ. 35 (2012) 234–244.
[51] A. Baxter, R. Mittler, N. Suzuki, ROS as key players in plant stress signalling, J. Exp. Bot. 65 (2014) 1229–1240.
[52] M.A. Torres, J.D.G. Jones, J.L. Dangl, Reactive oxygen species signaling in response to pathogens, Plant Physiol. 141 (2006) 373–378.
[53] N.P. Shetty, H.J.L. Jørgensen, J.D. Jensen, D.B. Collinge, H.S. Shetty, Roles of reactive oxygen species in interactions between plants and pathogens, Eur. J. Plant Pathol. 121 (2008) 267–280.
[54] M. Sagi, R. Fluhr, Superoxide production by the gp91phox NADPH oxidase plant homologue: modulation of activity by calcium and TMV, Plant Physiol. 126 (2001) 1281–1290.
[55] M.J. Curtis, T.J. Wolpert, The oat mitochondrial permeability transition and its implication in victorin binding and induced cell death, Plant J. 29 (2002) 295–312.
[56] M. Bras, B. Queenan, S.A. Susin, Programmed cell death via mitochondria: different modes of dying, Biochemistry 70 (2005) 231–239.
[57] A. Nogueira, L. Devin, M. Walter, X. Rigoulet, E. Leverve, Fontaine, Effects of decreasing mitochondrial volume on the regulation of the permeability transition pore, J. Bioenerg. Biomembr. 37 (2005) 25–33.
[58] D.M. Rhoads, C.S. Chalivendra, Mitochondrial retrograde regulation in plants, Mitochondrion 7 (2007) 177–194.
[59] N.P. Yurina, M.S. Odintsova, Signal transduction pathways of plant mitochondria: retrograde regulation, Russ J. Plant Physiol. 57 (2010) 7–19.
[60] A.G. Rasmusson, R.F. Alisdair, J.T. van Dongen, Alternative oxidase: a defence against metabolic fluctuations, Physiol. Plantarum 137 (2009) 371–382.
[61] Y.W.K. Liao, K. Shi, J.L. Fu, S. Zhang, X. Li, D.K. Dong, Y.P. Jiang, Y.H. Zhou, X.J. Xia, S.W. Liang, J.Q. Yu, The reduction of reactive oxygen species formation by mitochondrial alternative respiration in tomato basal defense against TMV Infection, Planta 235 (2012) 225–238.
[62] C. Norman, K.A. Howell, A.H. Millar, J.M. Whelan, D.A. Day, Salicylic acid is an uncoupler and inhibitor of mitochondrial electron transport, Plant Physiol. 134 (2004) 492–501.
[63] M. Cvetkovska, G.C. Vanlerberghe, Coordination of a mitochondrial superoxide burst during the hypersensitive response to bacterial pathogen in *Nicotiana tabacum*, Plant Cell Environ. 35 (2012) 1121–1136.
[64] M. Cvetkovska, G.C. Vanlerberghe, Alternative oxidase impacts the plant response to biotic stress by influencing the mitochondrial generation of reactive oxygen species, Plant Cell Environ. 36 (2013) 721–732.

[65] V.N. Popov, R.A. Simonian, V.P. Skulachev, A.A. Starkov, Inhibition of the alternative oxidase stimulates H_2O_2 production in plant mitochondria, FEBS Lett. 415 (1997) 87–90.
[66] D.P. Maxwell, R. Nickels, L. McIntosh, Evidence of mitochondrial involvement in the transduction of signals required for the induction of genes associated with pathogen attack and senescence, Plant J. 29 (2002) 269–279.
[67] G.C. Vanlerberghe, C.A. Robson, J.Y. Yip, Induction of mitochondrial alternative oxidase in response to a cell signal pathway down-regulating the cytochrome pathway prevents programmed cell death, Plant Physiol. 129 (2002) 1829–1842.
[68] J. Zarkovic, S.L. Anderson, D.M. Rhoads, A reporter gene system used to study developmental expression of alternative oxidase and isolate mitochondrial retrograde regulation mutants in Arabidopsis, Plant Mol. Biol. 57 (2005) 871–888.
[69] T. Kadono, D. Tran, R. Errakhi, T. Hiramatsu, P. Meimoun, M. Iwaya-inoue, T. Kawano, Increased anion channel activity is an unavoidable event in ozone-induced programmed cell death, Channels 5 (2010), http://dx.doi.org/10.1371/journal.pone.0013373
[70] S. Patel, J. Vemula, S. Konikkat, M.K. Barthwal, M. Dikshit, Ion channel modulators mediated alterations in NO-induced free radical generation and neutrophil membrane potential, Free Radic. Res. 43 (2009) 514–521.
[71] F.J. Maathuis, D. Sanders, Contrasting roles in ion transport of two K+ channel types in root cells of *Arabidopsis thaliana*, Planta 197 (1995) 456–464.
[72] D. Lecourieux, R. Ranjeva, A. Pugin, Calcium in plant defence-signalling pathways, New Phytol. 171 (2006) 249–269.
[73] P. Meimoun, D. Tran, M. Baz, R. Errakhi, A. Dauphin, A. Lehner, J. Briand, B. Biligui, K. Madiona, C. Beaulieu, F. Bouteau, Two different signaling pathways for thaxtomin A-induced cell death in Arabidopsis and tobacco BY2, Plant Signal. Behav. 4 (2009) 142–144.